SYNTHESIS AND CHARACTERIZATION OF GRAPHENE-ALUMINA NANOCOMPOSITE

Jong-Young Kim[1*], Jae-Ho Shin[1], Hyo-Jin Kim[1], Ungsoo Kim[1], Jae-Hwan Pee[1], Woo-seok Cho[1], Kyung Ja Kim[1]

[1]*Icheon Branch, Korea Institute of Ceramic Engineering and Technology, Icheon, Korea*
**e-mail address : jykim@kicet.re.kr*

Keywords: Graphene, Ceramic, Composite.

Abstract
We report synthesis of graphene-ceramic composite materials from graphene oxide (GO) or reduced graphene oxide (RGO) by thermal decomposition using alumina matrices. We incorporated GO and RGO in the ceramic matrices, and then densified using pressure-less sintering in inert atmosphere. Raman spectroscopic analysis showed that few layered graphene (FLG) with less than 5 layers was dispersed homogeneously in the matrix from the precursors of GO and RGO. Evidences of toughening mechanism such as sheet-pullout and crack bridging were observed from the microstructure of fracture surface, indicating that the graphene nanolayers could contribute the toughness of the composites. In addition, the encapsulated grapheme nanosheets around individual grains were shown to deflect the crack propagation, which could enhance the toughness of the composites.

1. Introduction

The exceptional mechanical, thermal, and electrical properties of graphene have prompted intense researches into a wide range of applications in structural materials, electronics, and energy management.[1-3] Attempts have been made to develop advanced engineering materials with improved properties through the incorporation of graphene in a matrix, however, most of the investigations on composites have so far focused on polymer-based composites with improved electrical and mechanical properties.[4] For example, the addition of graphene to a polymer matrix leads to a very low electrical percolation threshold and an improved electrical conductivity. [4] On the other hand, works have been much less focused on the composite in metal or ceramic matrices.

High Young's modulus of graphene (~1.0 TPa) makes it promising for reinforcement of ceramic matrix composite (CMC).[1] However, the following parameters were reported to be important for the reinforcement of the ceramic-graphene composite. First, the graphene nanosheet must be sufficiently bonded to the matrix so that they actually carry loads. Good interfacial bonding is required to achieve the load transfer across the graphene-matrix interface, which is a condition necessary for improving the mechanical properties of the ceramic composites. Second, the load must be distributed throughout the nanosheet to ensure that the outmost layer does not shear off. In principle, single walled carbon nanotube (SWCN) is preferred for making the composites of carbon nanotube (CNT) because the inner layers contribute little to carrying the load, and so it would reduce the stiffness for a given volume

fraction of the tubes.[5] However, as-prepared carbon nanotube tends to form bundles due to van der waals force, which causes strong aggregation of CNT in the matrix without an appropriate surface modification. When the above consideration on the reinforcement is applied, several advantages of graphene over CNT are expected. First, the graphene can be homogeneously dispersed throughout the matrix due to the hydrophilic surface of graphene oxide (GO), which can be readily reduced to graphene by chemical reduction or thermal treatment. Second, chemically or thermally reduced graphene layers still possess some functional group on the surface, which can be beneficial to strong bonding with the ceramic matrix. Third, the graphene materials can be produced in a large quantity by soft chemical route without expensive equipment and extreme experimental condition.

Ceramic matrix composite (CMC) conventionally uses one-dimensional fibers as reinforcement phases, such as carbon fiber,[6] carbon nanotube,[5,7] and ceramic whiskers.[8,9] Siegel et al. have reported that 24% improvement of fracture toughness over pure alumina can be obtained in 10.0 vol% MWCN-Al_2O_3 nanocomposite.[10] Zhan et al. reported a very large gain in fracture toughness to 9.7 $MPam^{1/2}$ in the alumina composites containing 10 vol% SWCN, which corresponds to nearly three times that of pure alumina.[5] Recently, the graphene and carbon nanotube have been considered as toughening materials in CMC containing alumina or silicon nitride, however, they suffered from thermal decomposition at high temperature and inhomogeneity due to an agglomeration of graphene and CNT.[11-13] They have fabricated fully dense nanocomposites of CNT or graphene with nanocrystalline alumina or silicon nitride by spark-plasma sintering, which was used to reduce structural damage of CNT and graphene due to long processing time at higher temperature in hot pressing method. Such decomposition problem and expensive process has prevented the carbon nanomaterials from industrial utilization.

In this work, we attempted to demonstrate the potential use of graphene in reinforcing the carbon-alumina composite. We have shown that the graphene-containing alumina composite can be prepared by employing in-situ formation from graphene oxide (GO) during sintering process in inert atmosphere, which were compared with the composites from reduced graphene oxide (RGO) by well-known chemical reduction of the exfoliated GO. The graphene-alumina composite materials can be obtained by sintering the slurry in inert atmosphere without any applied pressure and their mechanical properties were compared with respect to the process condition.

2. Results and Discussion

Raman scattering is strongly sensitive to the electronic structure and it has proved to be an essential tool to characterize the graphene materials. Figures 1(a)-1(e) show typical Raman spectra of raw graphite, GO samples prepared by Studenmaier method, reduced graphene oxide (RGO), 1.0 vol% graphene-alumina composite from GO precursor, and 1.0 vol% graphene-alumina composite from RGO precursor, respectively. In the spectra of pristine graphite, the peak at 1582 cm^{-1} (G band) corresponds to an E_{2g} mode of graphite and is related to the vibration of sp^2 bonded carbon atoms. The peak at 1352cm^{-1} (D band, the breathing mode of κ point phonons of A_{1g} symmetry) is associated with vibrations of carbon atoms with dangling bonds in plane terminations of disordered graphite. The Raman spectra suggest that the introduction of oxygen containing functional groups results in the change of hybridization of the oxidized carbon atoms from planar sp^2 to tetrahedral sp^3. The second order band (2D) is observed around 2700cm^{-1}. After the exfoliation, the D mode becomes stronger and broader because of a higher level of disorder of the graphene layers and defects increased during the

oxidation process. The G band shifted to 1591 cm^{-1} is well consistent with the previous result on the exfoliated GO.[14] Besides, compared to raw graphite, the ratio of the intensities (I_D/I_G) for GO samples is markedly increased, indicating the formation of sp^3 carbon by functionalization. This phenomenon can be also attributed to the significant decrease of the size of the in-plane sp^2 domains due to oxidation and ultrasonic exfoliation, and partially disordered graphite crystal structure of graphene nanosheets. After reduction by hydrazine, comparing with the graphite, the G band of reduced GO is shifted to 1573 cm^{-1} and D/G in intensity ratio has been slightly increased as shown in Figure 1(c). The present Raman results agree well with those reported by Stankovich, et al.[14] indicating the successful oxidation and exfoliation of graphite.

Raman spectra (Figures 1(d) and 1(e)) confirm that the graphene nanosheet is well-dispersed in the ceramic matrix and the sintered composites (1.0 vol% GO/RGO-alumina) undergo little or no damage to the graphene during ball milling and sintering process in inert atmosphere. The position of the 2D band varied in the order of raw graphite (2727 cm^{-1}) > RGO/GO (~2680 cm^{-1}), which may be attributed to the reason that the 2D-band position is down-shifted with a decreasing number of layers.[15] The 2D band (~2680 cm^{-1}) of the alumina composite indicates the thinning of the multilayered graphene into few layer graphene (FLG). When the GPL has less than 5 layers, the singlet 2D band can be distinguishable from multiplet of graphite in the previous result, which is well consistent with the present work. The position of G band (~1580 cm^{-1}) also supports few layer graphene (<5 layers) is dispersed in ceramic matrix.[16]

Figure 2(a) shows SEM image of fracture surfaces for the specimen of 100% alumina sintered at 1700℃. The cracks were produced by Vickers indentation, with a load of 98 N, in polished specimens. The area of the indent is approximately 150 μm^2. Clearly, the crack front propagated in an intergranular fracture mode. Figure 2(b) shows SEM image of fracture surfaces for 1.0 vol% graphene-alumina composites from GO precursor, sintered at 1500℃. It can be seen that the graphene nanosheets are fairly homogeneously dispersed in the matrix of alumina. The wrapping of the graphene along grain boundaries was observed, which could effectively entangle with the alumina grains to form a network structure.

Intimate contact between the graphene and the alumina grain was observed in fully dense materials, as shown in Figures 2(c) and 2(d), of 1.0 vol% graphene-alumina composites from GO and RGO precursors, respectively, sintered at 1700℃. It can be noted that the nanocomposite in Figure 2(b) exhibit a loose network with a lack of interfacial contact. On the other hand, a stronger bonding of graphene layers to the matrix can be observed in the nanocomposite, pressed by CIP (cold isostatic press) with 300MPa and sintered at higher temperature as shown in Figures 2(c) and 2(d). The features are quite different from alumina nanocomposites reinforced by carbon nanotubes grown in situ where the cohesion between the carbon nanotube and the matrix was poor and pull-out of CNT was observed.[5,10] The extent of interfacial bonding should be a factor in governing the toughness and strength of the composites.

Figure 2 indicates the presence of a variety of toughening mechanisms by graphene, including sheet pull-out, crack deflection, and crack bridging. Figures 2(c) and 2(d) show indentation crack profile on a polished surface in the 1.0 vol % graphene-alumina nanocomposite from GO and RGO precursors, respectively, sintered at 1700℃. Probing the crack wake in Figure

2(c), direct evidence of "pull-out" and graphene nanosheets that are bridging the cracks can be observed. The evidences of such toughening mechanisms as sheet pull-out or crack bridging are commonly observed in the propagated crack of the present composites. Such a crack bridging is also believed to result in an effective deflection of the propagated crack along the graphene/alumina interface as shown in Figure 2(d), which shows crack deflection results in a branched crack structure. It appears that the crack does not penetrate or puncture through the graphene nanosheets. When the large sheets of graphene running along the grain boundaries are located at the fracture surface, the graphene could prevent in-plane propagation of the crack, forcing the crack to change its propagation path and undergo out-of-plane deflection.[12]

Processing conditions, densities, and flexural strengths for the composites by solid state method and the liquid phase sintered composites are listed in Table 1. For the solid state method, the composites from GO and RGO exhibit practically the same flexural strength values. The GO-alumina composite by solid state shows a slight increase of flexural strength with increasing GO concentration from 0.25 vol % to 1.0 vol%. For the liquid phase sintering(LPS), the facture strength increases by ~40MPa compared to the composites by solid state method and the flexural strength shows remains the same with increasing GO concentration. The flexural strength for the composite from RGO precursor by LPS is lower by ~60MPa than the composite from GO.

Materials	Processing condition	Sintering Temp. (℃)	Density (g/cc)	Flexural strength σ_f (MPa)
Alumina	Solid state	1700	3.87	330.99±15.10
	LPS	1430	3.76	377.32±13.71
0.25 vol% GO	Solid state	1700	3.81	327.25±20.05
	LPS	1430	3.83	369.45±30.81
0.5 vol% GO	Solid state	1700	3.85	335.57±39.42
	LPS	1430	3.75	341.14±9.09
1.0 vol% GO	Solid state	1700	3.88	343.19±16.23
	LPS	1430	3.81	371.50±14.26
0.25 vol% RGO	Solid state	1700	3.80	324.16±15.39
	LPS	1430	3.76	310.08±26.43

Table 1. Processing conditions, densities, and flexural strengths for alumina-graphene composites.(LPS : liquid phase sintering, GO : graphene from graphene oxide precursor; RGO : graphene from reduced graphene oxide precursor)

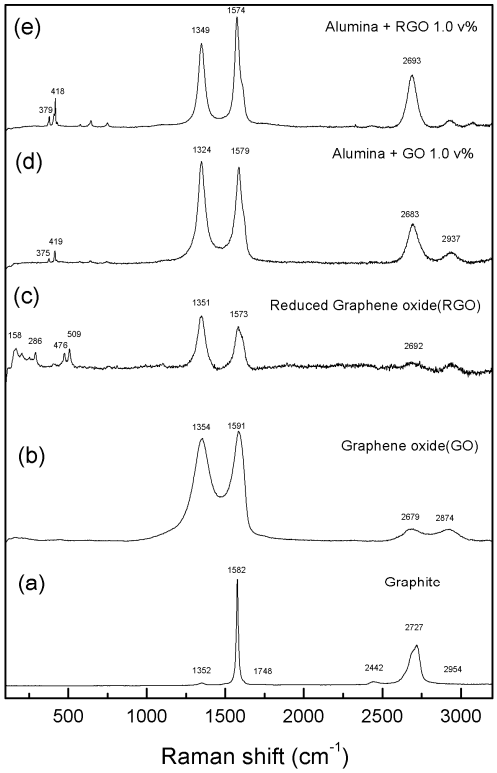

Figure 1. Raman spectra for (a) raw graphite, (b) graphene oxide, (c) reduced grapheme oxide, (d) 1.0 vol% graphene-alumina composite from GO, (e) 1.0 vol% graphene-alumina composite from RGO, respectively.

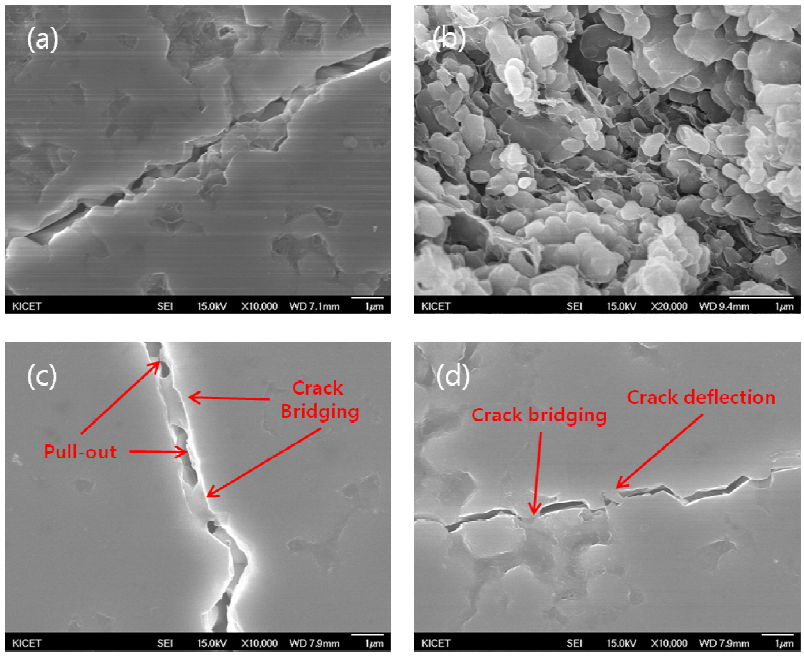

Figure 2. Crack profile for (a) pure alumina, (b) 1.0 vol% graphene-alumina composite from GO sintered at 1500℃, (c) 1.0 vol% graphene-alumina composite from GO sintered at 1700℃ (d) 1.0 vol% graphene-alumina composite from RGO sintered at 1700℃, respectively.

3. Materials and testing methods

Natural flake graphite, normally sized at 45μm, was provided by Aldrich. Fuming nitric acid (>90%), sulfuric acid (98%), potassium chlorate(98%) and hydrochloric acid(37%) were

purchased from Sigma-Aldrich and used as received. The graphene oxide (GO) was prepared according to the Staudenmaier method.[17,18] For homogeneous dispersion of graphene in the ceramic matrices, the following steps were taken. First, the GO prepared via the Staudenmaier method was exfoliated in water to produce a stable suspension of individual GO sheet using an ultrasonic bath. The GO suspension was exfoliated in de-ionized water with ultrasonic treatment for 30 min to form a colloidal suspension. The alumina slurry was prepared by mixing AES-11 (300nm, Sumitomo Co. Ltd) or glass-coated alumina for liquid phase sintering[19] with a dispersant and ball milling for 24 h to homogeneous slurries. Second, the aqueous slurries were added to the dispersed GO suspension and then ball-milled for 24 h using zirconia ball media. The volume percentage of GO was varied from 0.1 vol% to 1.0 vol% with the density of graphene (2.25 g/cm^3). When the composite of reduced graphene oxide was needed for comparison, the chemical reduction of GO with slurries by hydrazine hydrate was carried out.[14] Finally, the pressed compacts or casted body of the composite were sintered in electrical furnace to form graphene-alumina composite in Ar flowing atmosphere (3L/min). The transverse flexural strength (σ_f) was measured by the three-point-bending test on parallelepipedic specimens ($10 \times 10 \times 30$ mm^3) machined with a diamond blade. Universal tesing machine (UTM Inspekt table 250KN, Hegewald & Peschke) was used with load speed of 0.5mm/min. Final densities of the sintered compacts were determined by the Archimedes method with deionized water as immersion medium. Microstructure of the sintered specimens was examined by field emission scanning electron microscopy (FE-SEM).

4.References

[1] Yu M.-F., Files B. S., Arepalli S., Ruoff R. S. Tensile loading of ropes of single wall carbon nanotubes and their mechanical properties. *Phys. Rev. Lett.*, **84,** pp. 5552-5555 (2000). ; Lee C. G., Wei X. D., Kysar J. W. Hone J. Measurement of the elastic properties and intrinsic strength of monolayer grapheme. *Science,* **321**, pp. 385-388 (2008)_

[2] Novoselov K. S., Geim A. K., Morozov S. V., Jiang D., Zhang Y., Dubonos S. V., Grigorieva I. V., Firsov A. A. Electric field effect in atomically thin carbon films. *Science*, **306**, pp. 666-669(2004).

[3] Novoselov K. S., Jiang D., Schedin F., Booth T. J., Khotkevich V.V., Morozov S. V., Geim A. K. Two dimensional atomic crystals. *Proc. Natl. Acad. Sci.*, **102**, pp. 10451-10453(2005).

[4] Stankovich S., Dikin D. A., Dommett G.H.B., Kohlhaas K.M., Zimney E.J., Stach E. A., Piner R. D., Nguyen S. T., Ruoff R.S. Graphene-based composite materials. *Nature*, **442**, pp. 282-286(2006).

[5] Zhan G. D., Kuntz J. D., Wan J., Mukherjee A. K. Single-wall carbon nanotubes as attractive toughening agents in alumina-based nanocomposites. *Nature Mater*., **2**, pp. 38–42 (2002).

[6] Hyuga H., Jones M. I., Hirao K., Yamauchi Y. Fabrication and mechanical properties of Si_3N_4/Carbon fiber composites with aligned microstructure produced by a seeding and extrusion method. *J. Amer. Ceram. Soc*., **87**, pp. 894–899 (2004).

[7] Zhang T., Kumari L., Du G. H., Li W. Z., Wang Q. W., Balani K., Agarwal A. Mechanical properties of carbon nanotube-alumina nanocomposites synthesized by chemical vapor deposition and spark plasma sintering. *Compos. Part A*, **40**, pp. 86–93 (2009).

[8] Zhang P., Hu P., Zhang X., Han J., Meng, S. Processing and characterization of ZrB_2-SiCW ultra-high temperature ceramics. *J. Alloys Compd*., **472**, pp. 358–362 (2009).

[9] Zhang X., Xu L., Du S., Han W., Han, J. Crack-healing behavior of zirconium diboride composite reinforced with silicon carbide whiskers. *Scripta Mater.*, **59**, pp. 1222–1225 (2008)
[10] Siegel R.W., Chang S.K., Stone A.J., Ajayan P.M., Doremus R.W., Schadler L.S. Mechanical behavior of polymer and ceramic matrix nanocomposites. *Scripta Mater.*, **44,** pp. 2061–64 (2001).
[11] Wang X., Padture N. P., Tanaka H., Contact-damage-resistant ceramic/single-wall carbon nanotubes and ceramic/graphite composites. *Nature Mater.*, **3**, pp. 539-544 (2004)
[12] Walker L. S., Marotto V. R., Rafiee M. A., Koratkar N., Corral E. L., Toughening in graphene ceramic composites. *ACS Nano*, **5**, pp. 3182-3190 (2011)
[13] Wang K., Wang Y., Fan Z., Yan J., Wei T., Preparation of graphene nanosheet/alumina composites by spark plasma sintering, *Mater. Res. Bul.*, **46**, pp.315-318 (2011)
[14] Stankovich S., Dikin D. A., Piner R. D., Kohlhaas K. A., Kleinhammes A., Jia Y., Wu Y., Nguyen S. T., Ruoff R. S. Synthesis of graphene-based nanosheets via chemical reduction of exfoliated graphite oxide. *Carbon*, **45**, pp.1558-1565 (2007)
[15] Calizo I., Balandin A. A., Bao W., Miao F., Lau C. N. Temperature dependence of the Raman Spectra of graphene and graphene multilayers. *Nano Letters*, **7**, pp. 2645-2649 (2007); Gupta A., Chen G., Joshi P., Tadigadapa S., Eklund P. C. Raman scattering from high-frequency phonons in supported n-graphene layer films, *Nano Letters*, **6**, pp. 2667-2673 (2006); Ferrari A. C., Meyer J. C., Scardaci V., Casiraghi C., Lazzeri M., Mauri F., Piscanec S., Jiang D., Novoselov K. S., Roth S., Geim A. K., Raman Spectrum of Graphene and Graphene Layers, *Phys. Rev. Lett.*, **97**, pp.187401-187404 (2006)
[16] Kudin K. N., Ozbas B., Schniepp H. C., Prud'homme R. K., Aksay I. A., Car R., Raman Spectra of Graphite Oxide and Functionalized Graphene Sheets, *Nano Letters*, **8**, pp.36-41 (2008)
[17] Staudenmaier L. Verfahren zur Darstellung der Graphitsäure. *Ber. Dtsch. Chem. Ges.*, **31**, pp. 1481-1499(1898)
[18] Xu Y. X., Bai H., Lu G. W., Li C., Shi G. Q. Flexible graphene films via the filtration of water-soluble noncovalent functionalized graphene sheets. *J. Amer. Chem. Soc.* **130**, 5856(2008).
[19] Brydson R., Chen S.-C., Riley F. L., Milne S. J. Microstructure and chemistry of intergranular glassy films in liquid-phase-sintered alumina. *J. Amer. Cer. Soc.* **81**, 369-379(1998)